A novel S1PR4 functional antagonist prevents nonalcoholic steatohepatitis by deactivating the NLRP3 inflammasome without causing lymphopenia

Ki-Up Lee (kulee@amc.seoul.kr)
Asan Institute for Life Sciences, Asan Medical Center, University of Ulsan College of Medicine

Eun Hee Koh
Biomedical Research Center, Asan Institute for Life Sciences, Department of Internal Medicine, Asan Medical Center, University of Ulsan College of Medicine

Chung Hwan Hong
Asan Medical Center, University of Ulsan College of Medicine

Myoung Seok Ko
Asan Institute for Life Sciences, University of Ulsan College of Medicine

Jae Hyun Kim
College of Pharmacy, Seoul National University

Hyunkyung Cho
College of Pharmacy, Seoul National University

Chi-Ho Lee
College of Pharmacy, Gachon University

Ji Eun Yoon
Asan Medical Center, University of Ulsan College of Medicine

Ji-Young Yun
Biomedical Research Center, Asan Institute for Life Sciences, Asan Medical Center

In-Jeoung Baek
Univ of Ulsan College of Medicine / Asan Medical Center

Jung Eun Jang
Biomedical Research Center, Asan Institute for Life Sciences, Department of Internal Medicine, Asan Medical Center, University of Ulsan College of Medicine

Seung Eun Lee
Biomedical Research Center, Asan Institute for Life Sciences, Department of Internal Medicine, Asan Medical Center, University of Ulsan College of Medicine

Yun Kyung Cho
Asan Medical Center, University of Ulsan College of Medicine

Ji Yeon Baek

Asan Medical Center, University of Ulsan College of Medicine

Soo Jin Oh

New Drug Development Center, Asan Institute for Life Sciences, Asan Medical Center, University of Ulsan College of Medicine

Bong Yong Lee

Nextgen Bioscience

Joon Seo Lim

Asan Medical Center

Jongkook Lee

Kangwon National University

Sean Hartig

Baylor College of Medicine https://orcid.org/0000-0002-2695-2072

Jose Fernandez-Checa

Instituto Investigaciones Biomedicas de Barcelona

Ji Woong Choi

Gachon University

Sanghee Kim

College of Pharmacy, Seoul National University https://orcid.org/0000-0001-9125-9541

Article

Keywords: S1PR4, functional antagonist, NASH, inflammasome, Ca++

Posted Date: November 13th, 2020

DOI: https://doi.org/10.21203/rs.3.rs-96492/v1

Abstract

Sphingosine 1-phosphate (S1P) receptors (S1PRs) are a group of G protein-coupled receptors that confer a broad range of functional effects in chronic inflammatory diseases and metabolic diseases. S1PRs may also be involved in the development of non-alcoholic steatohepatitis (NASH), but the specific subtypes involved and the mechanism of action are unclear. Here we show that the livers of various mouse models of NASH as well as Kupffer cells had a particularly strong expression of S1pr4. Accordingly, genetic depletion of S1pr4 protected the mice against hepatic inflammation and fibrosis. Moreover, SLB736, a novel selective functional antagonist of SIPR4 prevented diet-induced NASH in mice without lymphopenia. S1P increased the expression of S1pr4 in Kupffer cells and activated the NLRP3 inflammasome through PLC/IP3/IP3R-dependent [Ca++] signaling. SLB736 treatment or S1pr4 depletion in Kupffer cells inhibited LPS-mediated Ca++ release and deactivated the NLRP3 inflammasome. S1PR4 antagonism may be a novel therapeutic strategy for NASH.

Introduction

Nonalcoholic fatty liver disease (NAFLD) has become a major health issue worldwide[1]. Approximately 10–20% of patients with NAFLD develop non-alcoholic steatohepatitis (NASH), an advanced stage of NAFLD that may subsequently progress to liver cirrhosis and hepatocellular carcinoma. The mechanism by which simple steatosis progresses to NASH and liver fibrosis is not completely understood, and an effective treatment for halting the progression of NASH is yet to be discovered[2,3].

Sphingosine 1-phosphate (S1P) is a bioactive sphingolipid that influences a wide range of important cellular processes by activating five G protein-coupled receptors (S1PR1-5)[4,5]. Receptor-mediated S1P signaling has become attractive therapeutic targets in several diseases such as chronic inflammatory disease, autoimmunity, cancer, and metabolic disease[6-10]. In the liver, S1PR2 participates in cholestasis-induced liver injury[11,12] and other causes of hepatic fibrosis[13]. S1PR1 and S1PR3 are involved in hepatic stellate cell motility and activation[14] and play a crucial role in the angiogenic process required for fibrosis development[15]. Targeting S1PRs was shown to be a promising strategy for treating NASH after the recent preclinical success of FTY720[16], a drug for multiple sclerosis[17]. FTY720 (Fingolimod; 2-amino-2-[2-(4-n-octylphenyl)ethyl]-1, 3-propanediol hydrochloride), a non-selective modulator of S1PRs (S1PR1, 3, 4, and 5), has been shown to prevent the development of alcoholic liver disease[18], NAFLD[19] and NASH[16] in murine models. However, a widespread use of FTY720 in NASH has been hampered by its lymphopenic effects.

In the present study, we have identified S1PR4 as a significant novel factor in the pathogenesis of NASH. We found that *S1pr4* mRNA expression was significantly high in the liver of various diet-induced murine models of NASH. *S1pr4* heterozygous knockout (*S1pr4*$^{+/-}$) mice were protected from high-fat, high-cholesterol diet (HFHCD)-induced NASH and hepatic fibrosis by showing minimal NLRP3 inflammasome activation in Kupffer cells. In order to provide further insights into the biological role of S1PR4, we

developed and characterized a S1PR4-selective modulator SLB736, which acted as a functional antagonist of S1PR4. SLB736 was effective in preventing the development of NASH and fibrosis via inhibiting the activation of NLRP3 inflammasome in Kupffer cells. Collectively, our results suggest that S1PR4 is a potential target for the treatment of NASH and hepatic fibrosis.

Results

Role of S1PR4 in the pathogenesis of NASH. We first investigated which type of S1PR isoforms is activated in the murine models of NASH. HFHCD-feeding is one of the animal models that closely resemble the clinical characteristics of NASH[1,20]. Despite its recognized effect in body weight[20,21], the methionine- and choline-deficient diet (MCDD) has long been used as a valuable model of NASH with respect to steatosis, inflammation, and fibrosis. Among other diet-induced murine models that closely resemble the clinical characteristics of NASH[21,22], we also used the Western diet (WD) and choline deficient, L-amino acid-defined, high-fat diet (CDA+HFD)[23]. Interestingly, S1PR4 was only the isoform that consistently showed increased mRNA expression in the livers of mice fed HFHCD, MCDD, WD, or CDA+HFD; the expression of *S1pr2 and S1pr1* were only increased in mice fed WD, and that of *S1pr3* expression was only increased in mice fed HFHCD or WD (Fig. 1a).

To address which cell types are responsible for this *S1pr4* upregulation, we examined the expression levels of *S1pr4* in primary hepatocytes, Kupffer cells, and hepatic stellate cells (HSC). *S1pr4* expression was rarely detected in hepatocytes and HSC; in contrast, *S1pr4* expression was significantly higher in Kupffer cells isolated from HFHCD-fed mice than those isolated from control mice (Fig. 1b, Supplementary Fig. 1).

S1PR4 was reported to be specifically expressed in myeloid cells such as dendritic cells and macrophages[24], but its role in the pathogenesis of NASH is largely unknown. We thus tested the possible involvement of S1PR4 in the development of NASH by using genetic modulation. As homozygous knockout of *S1pr4* resulted in embryonic lethality, we used heterozygous knockout (*S1pr4*$^{+/-}$) mice. Compared with HFHCD-fed WT mice, HFHCD-fed *S1pr4*$^{+/-}$ mice showed significantly lower degrees of hepatic inflammation and fibrosis (Fig. 1c-e); however, the degree of hepatic steatosis was similar regardless of the *S1pr4* genotype (Fig. 1c,f).

S1PR4 is necessary for the activation of NLRP3 inflammasome in Kupffer cells. NLRP3 inflammasome is involved in the pathogenesis of various inflammatory and metabolic diseases including arthritis, diabetes, and atherosclerosis[25-27]. Recent evidence also suggested that NLRP3 inflammasome activation in Kupffer cells is an important contributor to NASH and liver fibrosis[28], and NLRP3 inflammasome blockade by a small molecule was shown to reduce liver inflammation and fibrosis in experimental NASH in mice[29]. NLRP3 inflammasome is prominently expressed in Kupffer cells and moderately in HSC, and IL-1β produced by NLRP3 inflammasome promotes the proliferation and transdifferentiation of HSC to

induce liver fibrosis[30]. The first and the best-studied small molecule acting on S1PRs so far is FTY720, a myriocin-derived sphingolipid-like compound. Previous studies showed that FTY720 prevented the development of NASH[16]. Even though FTY720 affects multiple isoforms of S1PRs, S1PR1 is regarded as the main target of FTY720. Thus, in addition to S1PR4, S1PR1 may be a critical factor in NASH development. However, in our study, shRNA-mediated knockdown of *S1pr1* (Fig. 2a) did not significantly reduce the HFHCD-induced hepatic inflammation and fibrosis (Fig. 2b), nor did it significantly affect the markers for inflammation (Fig. 2c).

Kupffer cells from *S1pr4*$^{+/-}$ mice had a significantly lower degree of lipopolysaccharide (LPS)- and ATP-induced increases in interleukin-1β (IL-1β) production, whereas mice depleted of *S1pr1* by shRNA did not show significant differences from WT mice (Fig. 2d, e). These results suggest that *S1pr4*, but not *S1pr1*, is necessary for NLRP3 inflammasome activation in Kupffer cells. Collectively, these data indicate that S1PR4 is the critical mediator of the development of NASH.

SLB736 prevents the development of NASH and fibrosis. Administration of SLB736 to HFHCD-fed mice prevented the development of NASH and hepatic fibrosis (Fig. 4a, b) without affecting liver triglyceride (TG) levels (Fig. 4c). Interestingly, the administration of SLB736 did not reduce the number of lymphocytes, which is a well-known adverse effect of FTY720 through its effect on S1PR1[39,40] (Fig. 4d). Whereas treatment with SLB736 did not significantly reduce the diet-induced increases in the mRNA level of *S1pr4* (Fig. 4e), the protein level of S1PR4 was significantly decreased upon treatment with SLB736 (Fig. 4f), thus signifying that SLB736 carry functional antagonistic roles on S1PR4 *in vivo*.

We further investigated whether SLB736 shows a similar preventive effect in other diet-induced murine models of NASH. We found that similar to HFHCD-fed mice, mice fed MCDD or CDA+HFD developed NASH along with increases in the expression of inflammation and inflammasome markers, which were effectively nullified by the administration of SLB736 (Supplementary Fig. 3a-d). To further demonstrate the therapeutic effect of SLB736, we administered SLB736 to mice fed MCDD for 4 weeks, a time point at which hepatic steatosis was evident (Supplementary Fig. 3e). Administration of SLB736 for 4 weeks ameliorated NASH and fibrosis in these mice (Supplementary Fig. 3f).

-

S1PR4-dependent calcium release from ER plays a pivotal role in the priming of NLRP3 inflammasome in Kupffer cells. The activation of NLRP3 inflammasome is achieved through two sequential steps—signal 1 (priming) and signal 2 (activation)[41]: signal 1 is provided by microbial molecules or endogenous cytokines and leads to the upregulation of NLRP3 and pro-IL-1β through the activation of the transcription factor NF-kB, and signal 2 is triggered by ATP, pore-forming toxins, viral RNA, and particulate matters. Interestingly, we found that treatment with SLB736 significantly decreased IL-1β production in

Kupffer cells treated with LPS and ATP (Fig. 5a). Interestingly, SLB736 decreased the expression of *Nlrp3* and *Il-1β* (Fig. 5b) and the phosphorylation of NF-kB in LPS-primed primary Kupffer cells (Fig. 5c), suggesting that SLB736 inactivates the NLRP3 inflammasome from signal 1. Similarly, LPS-induced increases in *Nlrp3* and *IL-1β* were significantly nullified in *S1pr4*$^{+/-}$ Kupffer cells (Fig. 5d).

Intracellular ions such as K^+, Ca^{++}, and Cl^- have significant roles in the activation of the NLRP3 inflammasome[42]. Among them, intracellular Ca^{++} signaling plays one of the major roles in the activation of NLRP3 inflammasomes[43]. Accordingly, treatment with the [Ca^{++}] chelator BAPTA-AM in Kupffer cells significantly decreased the IL-1β production in response to LPS- and ATP-stimulation as well as the LPS-induced increases in the expression of *Nlrp3* and *IL-1β* (Fig. 5e, f).

Phospholipase C (PLC)-dependent changes in [Ca^{++}] are among the downstream signaling of various S1PRs[44]. Activation of PLC triggers the release of inositol trisphosphate (IP_3) from phosphatidylinositol 4, 5-bisphosphate (PIP_2), and [Ca^{++}] is released to the cytosol when IP_3 interacts with IP_3 receptor (IP_3R) located at the endoplasmic reticulum membrane[45]. In our experimental setting, treatment with PLC inhibitor U73122 or IP3R inhibitors Xes-c and 2-APB significantly decreased the LPS-mediated increases in the expression levels of *Nlrp3* and *Il-1β* (Fig. 5g, h) as well as the production of IL-1β in response to LPS- and ATP-stimulation (Fig. 5i). Taken together, these results indicate that increases in [Ca^{++}] release from the ER through the PLC/IP_3R axis play an important role in the activation of the NLRP3 inflammasome[43,46].

Measurement of [Ca^{++}] showed that LPS treatment in Kupffer cells or ATP treatment in LPS-primed Kupffer cells induced a robust increase in [Ca^{++}] (Fig. 6a,b, Supplementary Video 1, 2), which is in line with previously reported data[47]. Interestingly, pretreatment with SLB736 inhibited the LPS-induced [Ca^{++}] release in unprimed Kupffer cells but not the ATP-induced [Ca^{++}] release in LPS-primed Kupffer cells (Figure 6a, b, Supplementary Video 3, 4). Similarly, LPS-induced [Ca^{++}] release but not the ATP-induced [Ca^{++}] release in LPS-primed Kupffer cells was significantly decreased in *S1pr4*$^{+/-}$ Kupffer cells (Fig. 6c, d, Supplementary Video 5-8). Consistently, LPS-induced increase in the level of IP_3 (IP-one), the product of PLC[48], was significantly decreased in *S1pr4*$^{+/-}$ cells or cells treated with SLB736 (Fig. 6e, f). However, the ATP-induced increase in IP-one was not decreased in LPS-primed *S1pr4*$^{+/-}$ Kupffer cells or cells treated with SLB736 (Fig. 6g, h). These results collectively indicate that S1PR4 is required for the calcium signaling associated with signal 1 but not signal 2 of the NLRP3 inflammasome activation.

S1P activates the priming of NLRP3 inflammasome by the S1PR4/PLC/IP_3 axis. We examined the possible role of the S1P/S1PR4 axis in the priming of the NLRP3 inflammasome. Sphingosine kinase (SK) catalyzes the formation of S1P from the precursor sphingosine[4]. Interestingly, expression of *Sk1* was profoundly increased in the liver and in Kupffer cells but not in hepatocytes of HFHCD-fed mice (Fig. 7a-c). S1P significantly increased the expression level of *S1pr4* in Kupffer cells. S1P also significantly

increased the expression levels of *Nlrp3* and *Il-1β*, an effect that was dampened by pretreatment with SLB736 (Fig. 7d) and in *S1pr4*$^{+/-}$ Kupffer cells (Fig. 7e). S1P also stimulated the phosphorylation of NF-kB in Kupffer cells, and this was reduced by treatment with SLB736 (Fig. 7f) and in *S1pr4*$^{+/-}$ Kupffer cells (Fig. 7g). Pretreatment with BAPTA-AM, U73122, XesC, or 2-APB significantly reduced the S1P-mediated induction of *Nlrp3* and *Il-1β* expression (Fig. 7h). These results suggest that extracellular S1P may act as a paracrine modulator of the priming of the NLRP3 inflammasome in Kupffer cells through the PLC/IP_3/IP_3R signaling axis.

Discussion

S1PR4 is specifically expressed in myeloid cells such as dendritic cells and macrophages and regulates antigen-presenting cells to shape the T cell effector functions[49]. S1PR4 is also required for the differentiation of plasmacytoid dendritic cells[24] and regulates the production of interferon-α thereof[50]. However, compared with other S1PRs, our knowledge of the physiological relevance of S1PR4 has been modest[37]. In the present study, we found for the first time that S1PR4 in Kupffer cells plays an important role in the pathogenesis of NASH by activating the NLRP3 inflammasome. This is in line with a previous study that reported the upregulation of S1PR4 in human samples of liver cirrhosis[51].

As a major reservoir of intracellular [Ca^{++}], the ER plays a critical role in the regulation of intracellular [Ca^{++}] regulation[45]. Activation of the IP_3R, a Ca^{++}-release channel on the ER surface, is triggered by IP_3, a product of PLC-mediated PIP_2 cleavage. We found that LPS sequentially activated PLC and IP_3R in Kupffer cells to increase [Ca^{++}] and to activate the NLRP3 inflammasome, and that this reaction was abrogated by genetic depletion of *S1pr4* or treatment with SLB736. In addition to LPS, we found that S1P can also prime the NLRP3 inflammasome to activate it. Interestingly, expression of *Sk1* was induced in Kupffer cells by HFHCD feeding, and S1P increased the expression of *S1pr4* in Kupffer cells. Accordingly, a previous study showed that the overloading of saturated fatty acids induces *Sk1* in hepatocytes to initiate proinflammatory signaling[52]. On the other hand, in HFHCD-fed mice, *Sk1* expression was induced in Kupffer cells but not in hepatocytes. We thus suggest that S1P produced by SK1 from Kupffer cells induces S1PR4 in a paracrine manner to activate the NLRP3 inflammasome (Fig. 7i).

NAFLD occurs mostly in obese individuals, and insulin resistance and deregulation of the lipid metabolism increase the risk of NAFLD and NASH[1]. Although lifestyle modification is the first-line treatment for patients with NASH, it is usually unsuccessful. Therefore, many agents for the treatment of NASH by targeting different pathways are under development[2], and several compounds have shown promising histologic results in phase IIa studies[3,53]. However, it was pointed out that histologic NASH is not an independent predictor of long-term mortality and that the stage of fibrosis is the only robust and independent predictor of liver-related mortality[3,54]. In this regard, targeting the NLRP3 inflammasome activation, which plays a central role in hepatic inflammation and fibrosis[30], is increasingly recognized as a promising strategy for developing an efficient therapy against NASH[29,55,56]. In accordance, our study

showed that SLB736 was effective in preventing the development of NASH and fibrosis by deactivating the NLRP3 inflammasome.

One of the interesting findings is that treatment with SLB736 significantly mitigated hepatic inflammation or fibrosis while not significantly affecting the degree of hepatic steatosis. Similarly, *S1pr4*$^{+/-}$ mice did not show improvement in hepatic steatosis, despite the notable beneficial effects on inflammation and fibrosis. This suggests that S1PR4 specifically targets Kupffer cells and not hepatocytes. Lipotoxic hepatocyte injury may be the primary lesion that triggers the activation of NLRP3 inflammasome in Kupffer cells[57,58]. Thus, even though SLB736 shows promising effects on preventing hepatic inflammation and fibrosis, combination with other drugs that can reduce steatosis or lipotoxic injury of hepatocytes[2] may be more efficacious and may be used as an ideal therapy for the treatment of NASH.

Methods

SLB736. SLB736 was synthesized as a hydrochloride salt from according to the methods described in the Supplementary Methods. The chemical and spectroscopic data are as follows: m.p. 130°C; ^{1}H NMR (400 MHz, CD_3OD) δ 8.35 (s, 1H), 4.53 (t, J = 7.2 Hz, 2H), 3.69 (s, 4H), 2.97 (td, J = 4.3, 8.0 Hz, 2H), 2.11 (td, J = 4.3, 8.0 Hz, 2H), 2.00–1.95 (m, 2H), 1.35–1.28 (m, 14H), 0.89 (t, J = 6.8 Hz, 3H); ^{13}C NMR (100 MHz, CD_3OD) δ 146.5, 127.3, 63.0 (2C), 62.6, 54.3, 33.8, 32.0, 31.5, 31.4, 31.3, 31.2, 30.8, 28.1, 24.5, 19.9, 15.2; IR (neat) υ_{max} = 3180, 2918, 2851, 2421, 1599, 1454, 1080, 1063, 958, 715 (cm^{-1}); HRMS (FAB) calcd. for $C_{17}H_{35}N_4O_2$ $[M-Cl^-]^+$ 327.2760, found 327.2762 (Supplementary Fig. 2).

Mice and diet. Mice were housed in ambient temperature (22 ± 1°C) with a 12:12 h light-dark cycle and free access to water and food. After the indicated time of diet feeding, the mice were fasted for overnight before they were euthanized. All animal use and experiment protocols were approved by the Institutional Animal Care and Use Committee of Asan Institute for Life Sciences, Seoul, Korea.

Eight-weeks-old male C57BL/6J mice were fed either normal chow diet (ND; 12% energy from fat), CDA + HFD containing 60 kcal fat and 0.1% methionine (A06071302, Research Diets, New Brunswick, NJ) for 6 weeks, MCDD (Dyets Inc., Bethlehem, PA, USA) for 8 weeks, or HFHCD (60% energy from fat and 2.5% cholesterol, Dyets Inc.) for 12 weeks.

S1pr4 K/O mice were purchased from Jackson Laboratories (mouse strains, 005799; Bar Harbor, ME, USA). Because homozygous mutation of *S1pr4* results in mid-gestation embryonic lethality, *S1pr4*$^{+/-}$ mice were used. Littermate control (*S1pr4*$^{+/+}$) and *S1pr4*$^{+/-}$ mice were fed either ND or HFHCD.

Kupffer cells isolation and identification. Kupffer cells were isolated from mice by collagenase digestion, gradient centrifugation, and selective adherence,[59] with modifications. Briefly, the mice were anesthetized and the peritoneal cavity was opened; the livers were perfused with Ca^{++} and Mg^{++} free-Hank's balanced salt solution (HBSS) (LB 003-04, Welgene, Daegu, Korea) containing collagenase (17101-015, Gibco, Carlsbad, CA, USA) and trypsin inhibitor (T2011, Sigma-Aldrich, St. Louis, MO, USA). The digested livers

were removed and placed in 60-mm petri dishes. The livers were frittered with forceps in RPMI1640 (LM 011-01, Welgene) supplemented with 10% (vol/vol) FBS (16000-044, Gibco). The cell suspensions were filtered through a sterile 100-μm nylon cell strainer (352360, Falcon) to remove undigested tissues and connective tissues. The cells were centrifuged for 5 min at 50 × g at room temperature to remove hepatocytes. The supernatants were transferred to clean 50 ml tubes. The supernatants were centrifuged at 1600 rpm (4℃) for 10 min, and the cell pellets were re-suspended in 20% OptiPrep and gently layered on OptiPrep gradient (20, 11.5% and HBSS) and centrifuged at 3000 rpm at 4℃ for 17 min with the brake option off. Subsequently, the upper layers were removed and the cell fraction between 20% OptiPrep and 11.5% OptiPrep gradient were collected without contamination from the pellets. The collected layers were washed twice with RPMI1640 supplemented with 10% (vol/vol) FBS, and plated into 12-well or 24-well tissue culture plates. At 10 min after seeding, non-adherent cells (cell debris or blood cells) were removed by aspiration and fresh media were added. The next day, the cells were washed twice with 1 × PBS, and the attached Kupffer cells were cultured for another 48 h, at which point they were ready for experimental use.

Kupffer cells were identified by flow cytometry using a monoclonal anti-F4/80 antibody. Briefly, after 48 h of culture, Kupffer cells were detached by incubation with 0.25% trypsin for 5 min, and pelleted by centrifugation for 5 min at 100 rpm/min. The cells were then incubated with the anti-F4/80 antibody (clone BM8)-conjugated phycoerythrin (12-4801-82; Invitrogen, Carlsbad, CA, USA) for 30 min at 4℃ (1:200 dilution). The data were collected using the FACSCanto2 (BD Bioscience, San Jose, CA) and analyzed with the FlowJo software (Supplementary Fig. 1).

Primary HSC isolation. Selective macrophage depletion was achieved with a single intraperotoneal injection of clodronate (20 mg/ ml) according to manufacturer's instructions (FormuMax, Sunnyvale, CA, USA). After 24 hrs, primary HSCs were isolated using the same protocol used in the isolation of Kupffer cells, and the cell fraction between the upper layer and the 20% OptiPrep gradient were collected without contamination from the pellets. After centrifugation, the cells were seeded into culture plates in Dulbecco's modified Eagle's medium containing fetal serum at 37°C. The culture medium was changed and the RNA was isolated from primary HSCs[60].

Primary hepatocyte isolation and culture. Mice were perfused with HBSS (Welgene) pre-warmed in a 42°C water bath. Then, 0.36 mg/ml collagenase (Gibco) and trypsin inhibitor (Sigma-Aldrich) were added immediately before liver perfusion as previously described[61].

***S1pr1* shRNA-AAV tail vein injection.** Adeno-associated virus (AAV) vectors carrying *S1pr1* (AAV8-GFP-U6-m-S1PR1-shRNA, shAAV-271307) specific short hairpin RNA (shRNA) or scrambled shRNA (AAV8-GFP-U6-

scrmb shRNA, Control AAV: 5’-CAA CAA GAT GAA GAG CAC CAA CTC GAG TTG GTG CTC TTC ATC TTG TTG TTT TT-3’) were obtained from Vector Biolabs. The vectors were intravenously injected into the tail vein of 8-weeks-old C57BL/6J mice at a dose of 4×10^{11} plaque-forming units per mouse. Mice were fed HFHCD after the viral infection. After 6 weeks, the same dose was injected again.

Treatment with SLB736 or FTY720 *in vivo.* Mice were administrated SLB736, FTY720 (1 mg/kg body weight each) or vehicle (0.9% NaCl) via oral gavage every day for 5 days/week for the indicated periods. After the indicated period of treatment, the mice were fasted for overnight and sacrificed. The liver tissues were quickly removed and kept frozen at -70°C for subsequent analysis.

Histological analysis. Liver tissue samples were fixed in 10% neutral buffered formalin and embedded in paraffin. Serial sections (5 μm-thick) were stained with hematoxylin and eosin (H&E), Masson’s Trichrome (MT), or Sirius Red, as appropriate.

Liver TG contents. TG content in the liver was determined in duplicate using the Sigma Triglyceride (GPO-Trinder) kit.

SLB736 treatment *in vitro.* Cells were treated with chemicals at the indicated doses or sterile water (control) for 2 h. After washing twice with PBS, the cells were stimulated with LPS (L2880, Sigma-Aldrich) at a concentration of 100 ng/ml for 3 h, and then 1 mM ATP (A6419, Sigma-Aldrich) was added for 30 min.

Real-time PCR analysis. Total RNA isolated from each sample was reverse-transcribed and the target cDNA levels were quantified by real-time PCR analysis using gene-specific primers (Supplementary Table 1). Total RNA was isolated using TRIzol (Invitrogen), and 1 μg of each sample was reverse-transcribed with random primers using the Reverse Aid M-MuLV Reverse Transcription Kit (Fermentas, Amherst, NY, USA). The relative expression levels of each gene were normalized to that of 18S rRNA or *Tbp*.

Western blot analysis. Cell and liver samples were homogenized in lysis buffer (50 mM Tris, pH 7.4, 150 mM KCl, 4 mM EDTA, 4 mM EGTA and 1% NP-40 containing protease [04693132001, Roche, Carlsbad, CA, USA] and phosphatase [04906837001, Roche] inhibitor mixture tablets) at 4°C for 30 min. The resulting protein (40–50 μg) was subjected to immunoblotting with primary antibodies: antibodies against phosphorylated NF-kB (#3033) and NF-kB (#6956) were purchased from Cell Signaling (Danvers,

MA, USA) and the antibody against S1PR4 was purchased from NOVUS (NBP2-24500; Centennial, CO, USA). β-actin (A5441, Sigma-Aldrich) was used as housekeeping control (Supplementary Table 2). The signal intensities of protein bands were quantified with the ImageJ software (NIH, Bethesda, MD, USA) and normalized using the intensity of the loading control.

IL-1β measurement. Mouse IL-1β in cell culture supernatants were measured using the mouse IL-1β /IL-1F2 Quantikine ELISA kit (DY401, R&D Systems, Minneapolis, MN, USA).

Intracellular IP-one measurement. PLC activity was tested with the IP-one ELISA (72IP1PEA; Cisbio, Bedford, MA, USA), in which Kupffer cells were stimulated with LPS or S1P and then the cell culture medium was replaced with fresh medium. Intracellular IP-one, a surrogate measure for the level of inositol triphosphate, was measured after treatment with LiCl (50 mM) to prevent the degradation of IP-one into myo-inositol. The level of inositol triphosphate in cell lysates was measured using ELISA.

Determination of S1PR4 localization in C6 glioma cell line. Stable C6 glioma cells expressing EGFP-conjugated S1PR4 were prepared by infection with retrovirus bearing S1PR4-EGFP fusion construct (kindly provided by Dr. Jerold Chun at The Sanford Burnham Prebys). S1PR4 internalization and recycling were assessed as previously described[36]. In brief, cells were plated on poly-$_L$-lysine (100 mg/mL)-coated coverslips, cultivated, serum-deprived, and then used for experiments. The cells were treated with vehicle (0.1% fatty acid-free BSA), S1P, FTY720-P, or SLB736 for 0.5 h; in some cases, the cells were washed and further incubated in the presence of cycloheximide (5 mg/mL) for 2 h or 4 h. At the end of each experiment, the cells were fixed in 4% paraformaldehyde and mounted with Vectashield. S1PR4 localization in cells was assessed by detecting the EGFP signal using a laser scanning confocal microscopy (Eclipse A1+, Nikon, Tokyo, Japan).

S1PR β-Arrestin Assay. β-Arrestin recruitment assays for S1PR activity were performed by DiscoveRx (Fremont, CA, USA).

Calcium analysis by confocal microscopy. Kupffer cells were plated on 35 mm imaging dish (81156, Ibidi, Gräfelfing, Germany) at a density of 0.1×10^6 cells and incubated with Fluo-4/AM. Images of untreated cells were acquired at t = 0, and the cells were treated with 1 mg/ml LPS or 1 mM ATP in RPMI 1640. The cells were imaged for 5 min at 5 s intervals on a Zeiss LSM780 Confocal Imaging System using the 488 nm laser and emission in the range of 500–600 nm. The images were analyzed using Zen 2012 SP5

software by creating surfaces to encompass the volume of each cell. The absolute intensity for all cells in a field at different time points was obtained, and normalized to t=0 to calculate the fold increases in intensity. Data are displayed as the relative intensity of cells in a field.

Blood lymphocyte measurement. Blood lymphocytes were counted using an automated hematology analyzer (ADVIA 2120i 53, Siemens Healthcare Diagnostics, Tarrytown, NY, USA).

Reagents for calcium signaling. BAPTA-AM (A1076, Sigma-Aldrich), U73122 (U6756, Sigma-Aldrich), 2-APB (D9754, Sigma-Aldrich), and Xes-c (X2628, Sigma-Aldrich) were used for detecting calcium signaling.

Statistical analysis. Data are expressed as mean ± standard error of the mean (SEM). Unpaired two-tailed Student's *t*-tests were used to compare variables between groups, and one-way ANOVA was used to compare variables among multiple groups. For the comparison of multiple measurements made at different time points, one-way repeated-measures ANOVA was used. Bonferroni correction was applied for post hoc analysis of the multiple comparisons. All statistical tests were conducted according to two-sided sample sizes and were determined on the basis of previous experiments that used similar methodologies. For all experiments, the stated replicates are biological replicates. Statistical analysis and graphing were performed using IBM SPSS Statistics for Windows version 22.0 (IBM Corp., Armonk, NY, USA) or GraphPad Prism 7 (GraphPad Software, La Jolla, CA, USA).

References

1. Friedman, S. L., Neuschwander-Tetri, B. A., Rinella, M. & Sanyal, A. J. Mechanisms of NAFLD development and therapeutic strategies. *Nat Med* **24**, 908-922 (2018).
2. Lassailly, G., Caiazzo, R., Pattou, F. & Mathurin, P. Perspectives on Treatment for Nonalcoholic Steatohepatitis. *Gastroenterology* **150**, 1835-1848 (2016).
3. Younossi, Z. M. *et al.* Current and future therapeutic regimens for nonalcoholic fatty liver disease and nonalcoholic steatohepatitis. *Hepatology* **68**, 361-371 (2018).
4. Cartier, A. & Hla, T. Sphingosine 1-phosphate: Lipid signaling in pathology and therapy. *Science* **366** (2019).
5. Blaho, V. A. & Hla, T. An update on the biology of sphingosine 1-phosphate receptors. *Journal of lipid research* **55**, 1596-1608 (2014).
6. Ng, M. L., Wadham, C. & Sukocheva, O. A. The role of sphingolipid signalling in diabetesassociated pathologies (Review). *Int J Mol Med* **39**, 243-252 (2017).

7. Wang, F. *et al.* Sphingosine-1-phosphate receptor-2 deficiency leads to inhibition of macrophage proinflammatory activities and atherosclerosis in apoE-deficient mice. *J Clin Invest* **120**, 3979-3995 (2010).
8. Lee, S. Y. *et al.* Activation of sphingosine kinase 2 by endoplasmic reticulum stress ameliorates hepatic steatosis and insulin resistance in mice. *Hepatology* **62**, 135-146 (2015).
9. Ogretmen, B. Sphingolipid metabolism in cancer signalling and therapy. *Nat Rev Cancer* **18**, 33-50 (2018).
10. Tsai, H. C. & Han, M. H. Sphingosine-1-Phosphate (S1P) and S1P Signaling Pathway: Therapeutic Targets in Autoimmunity and Inflammation. *Drugs* **76**, 1067-1079 (2016).
11. Wang, Y. *et al.* The role of sphingosine 1-phosphate receptor 2 in bile-acid-induced cholangiocyte proliferation and cholestasis-induced liver injury in mice. *Hepatology* **65**, 2005-2018 (2017).
12. Xiao, Y. *et al.* Long Noncoding RNA H19 Contributes to Cholangiocyte Proliferation and Cholestatic Liver Fibrosis in Biliary Atresia. *Hepatology* **70**, 1658-1673 (2019).
13. Hou, L. *et al.* Macrophage Sphingosine 1-Phosphate Receptor 2 Blockade Attenuates Liver Inflammation and Fibrogenesis Triggered by NLRP3 Inflammasome. *Front Immunol* **11**, 1149 (2020).
14. Liu, X. *et al.* Essential roles of sphingosine 1-phosphate receptor types 1 and 3 in human hepatic stellate cells motility and activation. *J Cell Physiol* **226**, 2370-2377 (2011).
15. Yang, L. *et al.* Sphingosine kinase/sphingosine 1-phosphate (S1P)/S1P receptor axis is involved in liver fibrosis-associated angiogenesis. *J Hepatol* **59**, 114-123 (2013).
16. Mauer, A. S., Hirsova, P., Maiers, J. L., Shah, V. H. & Malhi, H. Inhibition of sphingosine 1-phosphate signaling ameliorates murine nonalcoholic steatohepatitis. *Am J Physiol Gastrointest Liver Physiol* **312**, G300-G313 (2017).
17. Calabresi, P. A. *et al.* Safety and efficacy of fingolimod in patients with relapsing-remitting multiple sclerosis (FREEDOMS II): a double-blind, randomised, placebo-controlled, phase 3 trial. *Lancet Neurol* **13**, 545-556 (2014).
18. Moro-Sibilot, L. *et al.* Mouse and Human Liver Contain Immunoglobulin A-Secreting Cells Originating From Peyer's Patches and Directed Against Intestinal Antigens. *Gastroenterology* **151**, 311-323 (2016).
19. Rohrbach, T. D. *et al.* FTY720/fingolimod decreases hepatic steatosis and expression of fatty acid synthase in diet-induced nonalcoholic fatty liver disease in mice. *J Lipid Res* **60**, 1311-1322 (2019).
20. Jang, J. E. *et al.* Protective role of endogenous plasmalogens against hepatic steatosis and steatohepatitis in mice. *Hepatology* **66**, 416-431 (2017).
21. Farrell, G. *et al.* Mouse Models of Nonalcoholic Steatohepatitis: Toward Optimization of Their Relevance to Human Nonalcoholic Steatohepatitis. *Hepatology* **69**, 2241-2257 (2019).
22. Santhekadur, P. K., Kumar, D. P. & Sanyal, A. J. Preclinical models of non-alcoholic fatty liver disease. *J Hepatol* **68**, 230-237 (2018).

23. Matsumoto, M. *et al.* An improved mouse model that rapidly develops fibrosis in non-alcoholic steatohepatitis. *International journal of experimental pathology* **94**, 93-103 (2013).
24. Dillmann, C., Mora, J., Olesch, C., Brune, B. & Weigert, A. S1PR4 is required for plasmacytoid dendritic cell differentiation. *Biol Chem* **396**, 775-782 (2015).
25. Strowig, T., Henao-Mejia, J., Elinav, E. & Flavell, R. Inflammasomes in health and disease. *Nature* **481**, 278-286 (2012).
26. Davis, B. K., Wen, H. & Ting, J. P. The inflammasome NLRs in immunity, inflammation, and associated diseases. *Annu Rev Immunol* **29**, 707-735 (2011).
27. Schroder, K., Zhou, R. & Tschopp, J. The NLRP3 inflammasome: a sensor for metabolic danger? *Science* **327**, 296-300 (2010).
28. Knorr, J., Wree, A., Tacke, F. & Feldstein, A. E. The NLRP3 Inflammasome in Alcoholic and Nonalcoholic Steatohepatitis. *Semin Liver Dis* **40**, 298-306 (2020).
29. Mridha, A. R. *et al.* NLRP3 inflammasome blockade reduces liver inflammation and fibrosis in experimental NASH in mice. *J Hepatol* **66**, 1037-1046 (2017).
30. Alegre, F., Pelegrin, P. & Feldstein, A. E. Inflammasomes in Liver Fibrosis. *Semin Liver Dis* **37**, 119-127 (2017).
31. Hanson, M. A. *et al.* Crystal structure of a lipid G protein-coupled receptor. *Science* **335**, 851-855 (2012).
32. Pham, T. C. *et al.* Molecular recognition in the sphingosine 1-phosphate receptor family. *J Mol Graph Model* **26**, 1189-1201 (2008).
33. Oo, M. L. *et al.* Immunosuppressive and anti-angiogenic sphingosine 1-phosphate receptor-1 agonists induce ubiquitinylation and proteasomal degradation of the receptor. *J Biol Chem* **282**, 9082-9089 (2007).
34. Graler, M. H. & Goetzl, E. J. The immunosuppressant FTY720 down-regulates sphingosine 1-phosphate G-protein-coupled receptors. *FASEB J* **18**, 551-553 (2004).
35. O'Sullivan, C., Schubart, A., Mir, A. K. & Dev, K. K. The dual S1PR1/S1PR5 drug BAF312 (Siponimod) attenuates demyelination in organotypic slice cultures. *J Neuroinflammation* **13**, 31 (2016).
36. Choi, J. W. *et al.* FTY720 (fingolimod) efficacy in an animal model of multiple sclerosis requires astrocyte sphingosine 1-phosphate receptor 1 (S1P1) modulation. *Proc Natl Acad Sci U S A* **108**, 751-756 (2011).
37. Stepanovska, B. & Huwiler, A. Targeting the S1P receptor signaling pathways as a promising approach for treatment of autoimmune and inflammatory diseases. *Pharmacol Res*, 104170 (2019).
38. Garris, C. S., Blaho, V. A., Hla, T. & Han, M. H. Sphingosine-1-phosphate receptor 1 signalling in T cells: trafficking and beyond. *Immunology* **142**, 347-353 (2014).
39. Matloubian, M. *et al.* Lymphocyte egress from thymus and peripheral lymphoid organs is dependent on S1P receptor 1. *Nature* **427**, 355-360 (2004).

40. Enriquez-Marulanda, A. *et al.* Cerebral toxoplasmosis in an MS patient receiving Fingolimod. *Mult Scler Relat Disord* **18**, 106-108 (2017).
41. He, Y., Hara, H. & Nunez, G. Mechanism and Regulation of NLRP3 Inflammasome Activation. *Trends Biochem Sci* **41**, 1012-1021 (2016).
42. Gong, T., Yang, Y., Jin, T., Jiang, W. & Zhou, R. Orchestration of NLRP3 Inflammasome Activation by Ion Fluxes. *Trends Immunol* **39**, 393-406 (2018).
43. Lee, G. S. *et al.* The calcium-sensing receptor regulates the NLRP3 inflammasome through Ca2+ and cAMP. *Nature* **492**, 123-127 (2012).
44. Sanchez, T. & Hla, T. Structural and functional characteristics of S1P receptors. *J Cell Biochem* **92**, 913-922 (2004).
45. Raffaello, A., Mammucari, C., Gherardi, G. & Rizzuto, R. Calcium at the Center of Cell Signaling: Interplay between Endoplasmic Reticulum, Mitochondria, and Lysosomes. *Trends Biochem Sci* **41**, 1035-1049 (2016).
46. Murakami, T. *et al.* Critical role for calcium mobilization in activation of the NLRP3 inflammasome. *Proc Natl Acad Sci U S A* **109**, 11282-11287 (2012).
47. Schappe, M. S. *et al.* Chanzyme TRPM7 Mediates the Ca(2+) Influx Essential for Lipopolysaccharide-Induced Toll-Like Receptor 4 Endocytosis and Macrophage Activation. *Immunity* **48**, 59-74 e55 (2018).
48. Chiang, C. Y., Veckman, V., Limmer, K. & David, M. Phospholipase Cgamma-2 and intracellular calcium are required for lipopolysaccharide-induced Toll-like receptor 4 (TLR4) endocytosis and interferon regulatory factor 3 (IRF3) activation. *J Biol Chem* **287**, 3704-3709 (2012).
49. Olesch, C., Ringel, C., Brune, B. & Weigert, A. Beyond Immune Cell Migration: The Emerging Role of the Sphingosine-1-phosphate Receptor S1PR4 as a Modulator of Innate Immune Cell Activation. *Mediators of inflammation* **2017**, 6059203 (2017).
50. Dillmann, C. *et al.* S1PR4 Signaling Attenuates ILT 7 Internalization To Limit IFN-alpha Production by Human Plasmacytoid Dendritic Cells. *Journal of immunology* **196**, 1579-1590 (2016).
51. Kim, K. M. *et al.* Galpha12 overexpression induced by miR-16 dysregulation contributes to liver fibrosis by promoting autophagy in hepatic stellate cells. *J Hepatol* **68**, 493-504 (2018).
52. Geng, T. *et al.* SphK1 mediates hepatic inflammation in a mouse model of NASH induced by high saturated fat feeding and initiates proinflammatory signaling in hepatocytes. *J Lipid Res* **56**, 2359-2371 (2015).
53. Konerman, M. A., Jones, J. C. & Harrison, S. A. Pharmacotherapy for NASH: Current and emerging. *Journal of hepatology* **68**, 362-375 (2018).
54. Taylor, R. S. *et al.* Association Between Fibrosis Stage and Outcomes of Patients With Nonalcoholic Fatty Liver Disease: A Systematic Review and Meta-Analysis. *Gastroenterology* (2020).
55. Tilg, H., Moschen, A. R. & Szabo, G. Interleukin-1 and inflammasomes in alcoholic liver disease/acute alcoholic hepatitis and nonalcoholic fatty liver disease/nonalcoholic steatohepatitis. *Hepatology* **64**,

955-965 (2016).

56. Petrasek, J. *et al.* IL-1 receptor antagonist ameliorates inflammasome-dependent alcoholic steatohepatitis in mice. *J Clin Invest* **122**, 3476-3489 (2012).
57. Machado, M. V. & Diehl, A. M. Pathogenesis of Nonalcoholic Steatohepatitis. *Gastroenterology* **150**, 1769-1777 (2016).
58. Farrell, G. C., Haczeyni, F. & Chitturi, S. Pathogenesis of NASH: How Metabolic Complications of Overnutrition Favour Lipotoxicity and Pro-Inflammatory Fatty Liver Disease. *Adv Exp Med Biol* **1061**, 19-44 (2018).
59. Li, P. Z., Li, J. Z., Li, M., Gong, J. P. & He, K. An efficient method to isolate and culture mouse Kupffer cells. *Immunol Lett* **158**, 52-56 (2014).
60. Inzaugarat, M. E. *et al.* NLR Family Pyrin Domain-Containing 3 Inflammasome Activation in Hepatic Stellate Cells Induces Liver Fibrosis in Mice. *Hepatology* **69**, 845-859 (2019).
61. Mitaka, T. The current status of primary hepatocyte culture. *Int J Exp Pathol* **79**, 393-409 (1998).

Declarations

Acknowledgements

This study was supported by grants from the following organizations: the National Research Foundation of Korea (NRF), funded by the Ministry of Education, Science, and Technology, Korea (2017R1E1A1A01073206: K.-U.L., 2017R1E1A1A01074207: E.H.K), the Korea Drug Development Fund (KDDF) funded by the Ministry of Science and ICT, Ministry of Trade, Industry & Energy, and Ministry of Health & Welfare (KDDF-201406-03: K.-U.L., Republic of Korea), and Asan Institute for Life Sciences, Korea (2020IP0016-1). This work was also supported by the Mid-Career Researcher Programs (NRF-2019R1A2C2009905: S.K.) of the National Research Foundation of Korea (NRF) grant funded by the Government of Korea (MSIP). We acknowledge support from grant PID2019-111669RB from Plan Nacional de I+D, Spain, by the CIBEREHD, Instituto de Salud Carlos III, Spain; the Center grant P50AA011999 Southern California Research Center for ALPD and Cirrhosis funded by NIAAA; support from AGAUR of the Generalitat de Cataluña SGR-2017-1112 and the “ER stress-mitochondrial cholesterol axis in obesity-associated insulin resistance and comorbidities”-Ayudas Fundación BBVA a Equipos de Investigación Científica 2017 and the Red Nacional 2018-102799-T de Enfermedades Metabólicas y Cáncer, the Project 201916/31 Contribution of mitochondrial oxysterol and bile acid metabolism to liver carcinogenesis 2019 by Fundació Marato TV3.

Author contributions

E.H.K. conceptualized and designed the study and wrote the manuscript. C.H.H. designed the study and performed the *in vitro* and *in vivo* molecular experiments. M.S.K. performed *in vitro* and molecular experiments. J.H.K. and H.C. designed and constructed all chemical compounds. J.Y.Y. performed the *in*

vivo experiments. J.E.Y. performed the *in vitro* experiments. J.E.J., S.E.L., Y.K.C., J.Y.B., J.S.L., S.J.O., B.I.J., and B.Y.L. critically reviewed the manuscript, provided suggestions, and contributed to the discussion. J.L. contributed to the construction of chemicals. C.L. and J.W.C. performed the *in vitro* S1PR activity experiments. S.H., J.S.L., and J.C.F.C. critically reviewed the manuscript. S.K. designed all chemical compounds. J.W.C., S.K., and K.-U.L. conceptualized the study, wrote the manuscript, and are responsible for the integrity of this work as corresponding authors. All authors discussed the results and commented on the manuscript.

Conflicts of interest

E.H.K., S.K., and K.-U.L. have filed a provisional patent application in the Korea patent office as application No. 10-2017-00040139: “Composition for preventing and treating nonalcoholic steatohepatitis by targeting S1PR4.”

Figures

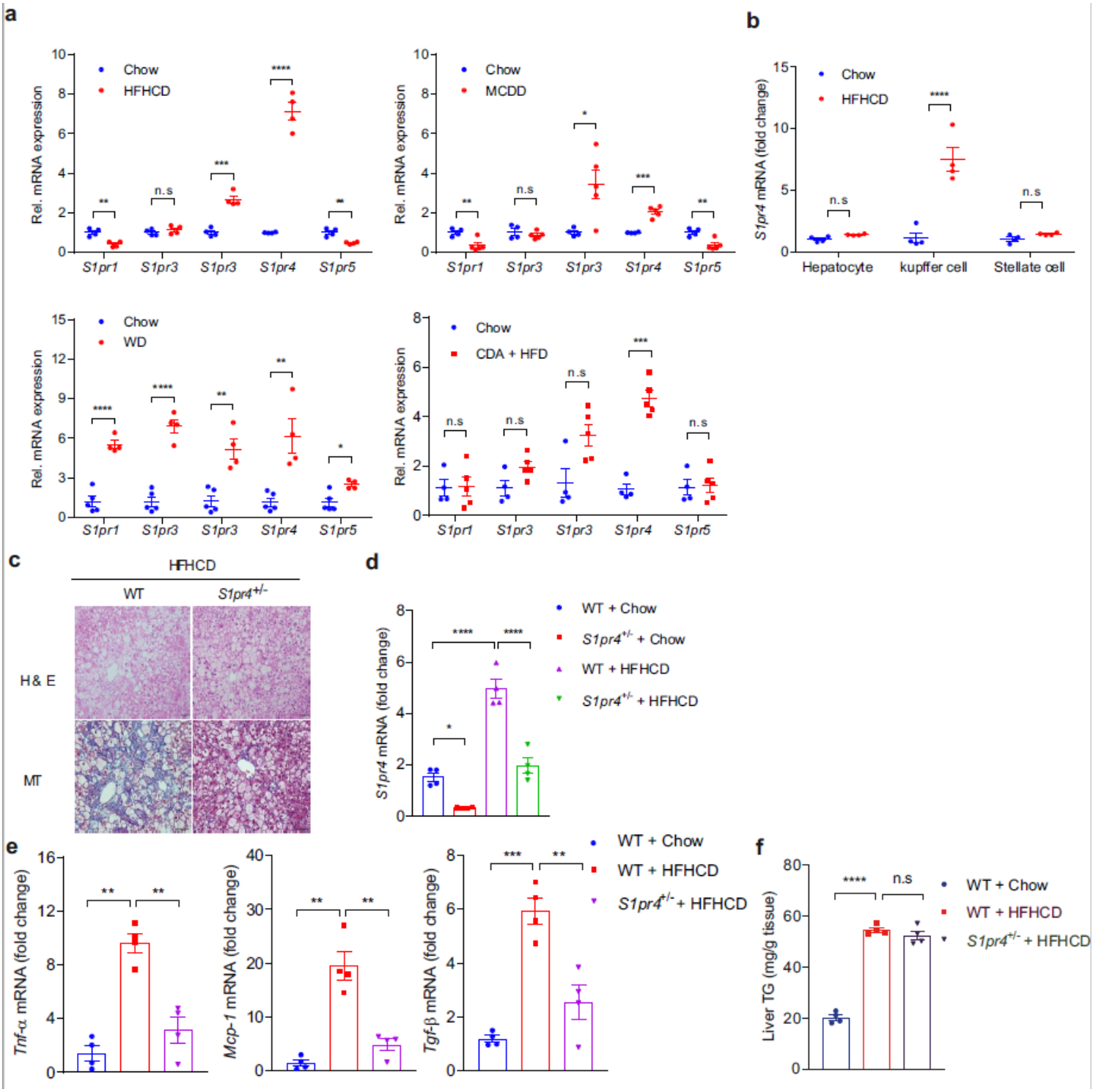

Figure 1

S1PR4 is an important mediator of the development of NASH. a S1pr4 expression is specifically increased in mouse models of NASH. Hepatic S1pr mRNA expression in HFHCD-, MCDD-, WD- and CDA+HFD-induced dietary models of NASH (n = 4-5). b mRNA expression of S1prs in primary hepatocytes, Kupffer cells, and HSCs from mice fed chow diet (Con) or HFHCD for 4 weeks (n = 4). c-f S1PR4 knockout prevents the development of NASH. S1pr4+/- mice were fed chow diet or HFHCD for 12 weeks. c Representative H&E and MT staining in liver tissues. Scale bar, 50 μm. d Hepatic mRNA

expression levels of S1pr4 (n = 4). e Relative mRNA expression levels of the genes associated with the inflammation and fibrosis (n = 4). f Liver TG contents (n = 4). All data are shown as mean ± SEM. Data in a, b were analyzed by unpaired t-test. Data in d-f were analyzed by one-way ANOVA followed by Tukey's multiple comparisons test. *p < 0.05, **p < 0.01, ***p < 0.001, ****p < 0.0001, n.s, not significant.

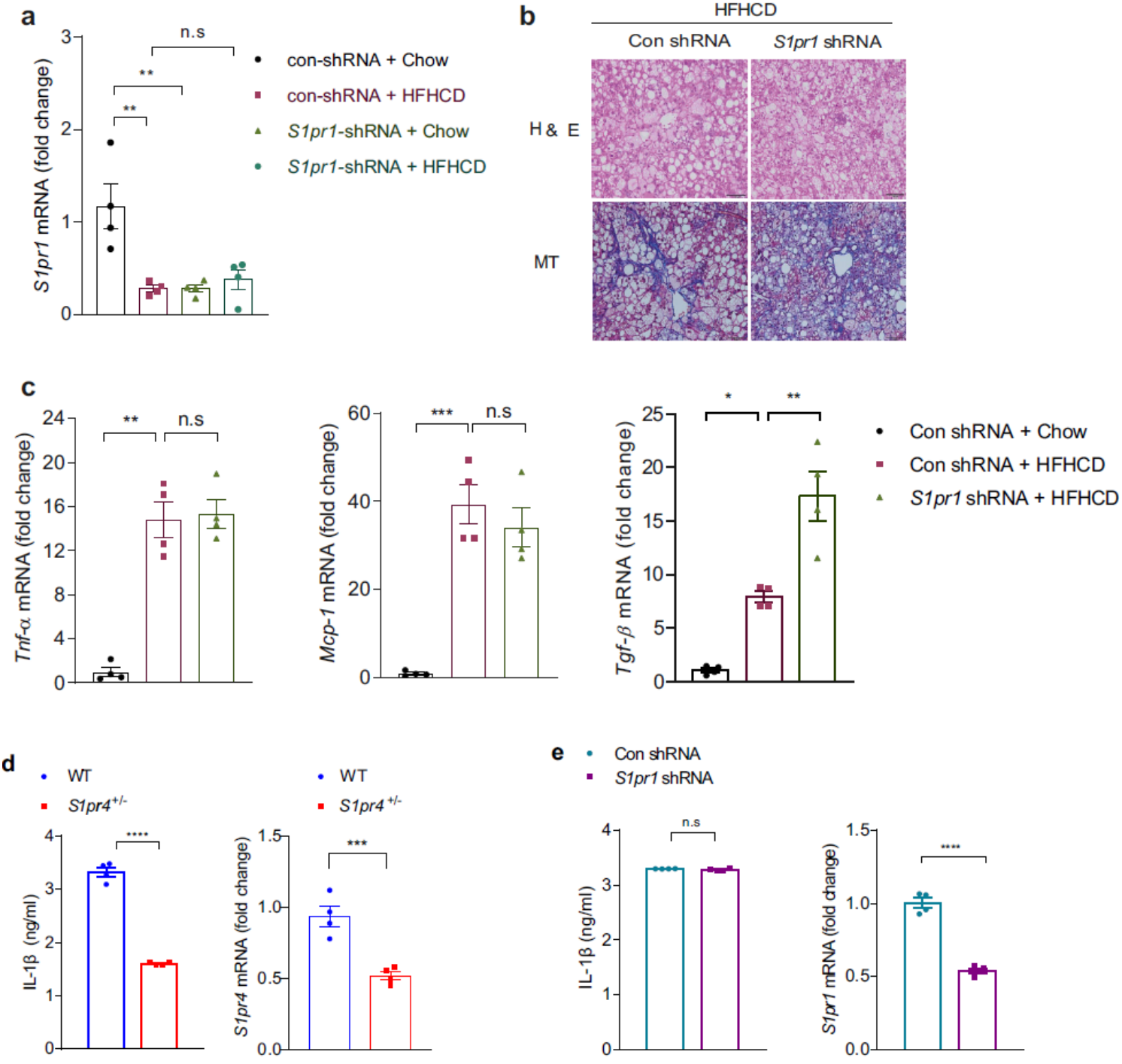

Figure 2

S1PR4, not S1PR1, is necessary for the activation of NLRP3 inflammasome in macrophages. a-d S1pr1 knockdown does not prevent the development of NASH. Mice were infected with AAV carrying control (shCon) or S1pr1-specific shRNA (shS1pr1), and then fed ND or HFHCD for 12 weeks. a Hepatic mRNA expression levels of S1pr1. b Representative H&E and MT staining in liver tissues. Scale bar, 50 μm. c

Relative mRNA expression levels of the genes associated with inflammation and fibrosis (n = 4). d, e Depletion of S1pr4 but not S1pr1 decreases the activation of NLRP3 inflammasomes in liver macrophages. To knockdown S1pr1 in Kupffer cells, male C57BL/6J mice were injected with AAV-Control or AAV-shS1pr1, and then the Kupffer cells were isolated four weeks after (n = 4) (e). Kupffer cells isolated from S1pr4 +/- mice and S1pr1-knockdown mice were stimulated with LPS (100 ng/ml) for 3 h followed by ATP (1 mM) for 30 min. Cell culture media were collected and the IL-1β levels were measured by ELISA (n = 4). Data are shown as mean ± SEM. Data in a and c were analyzed by one-way ANOVA followed by Tukey's multiple comparisons test. Data in d and e were analyzed by two-tailed Student's t-test. *p < 0.05, **p < 0.01, ***p <0.001, ****p <0.001, n.s; not significant.

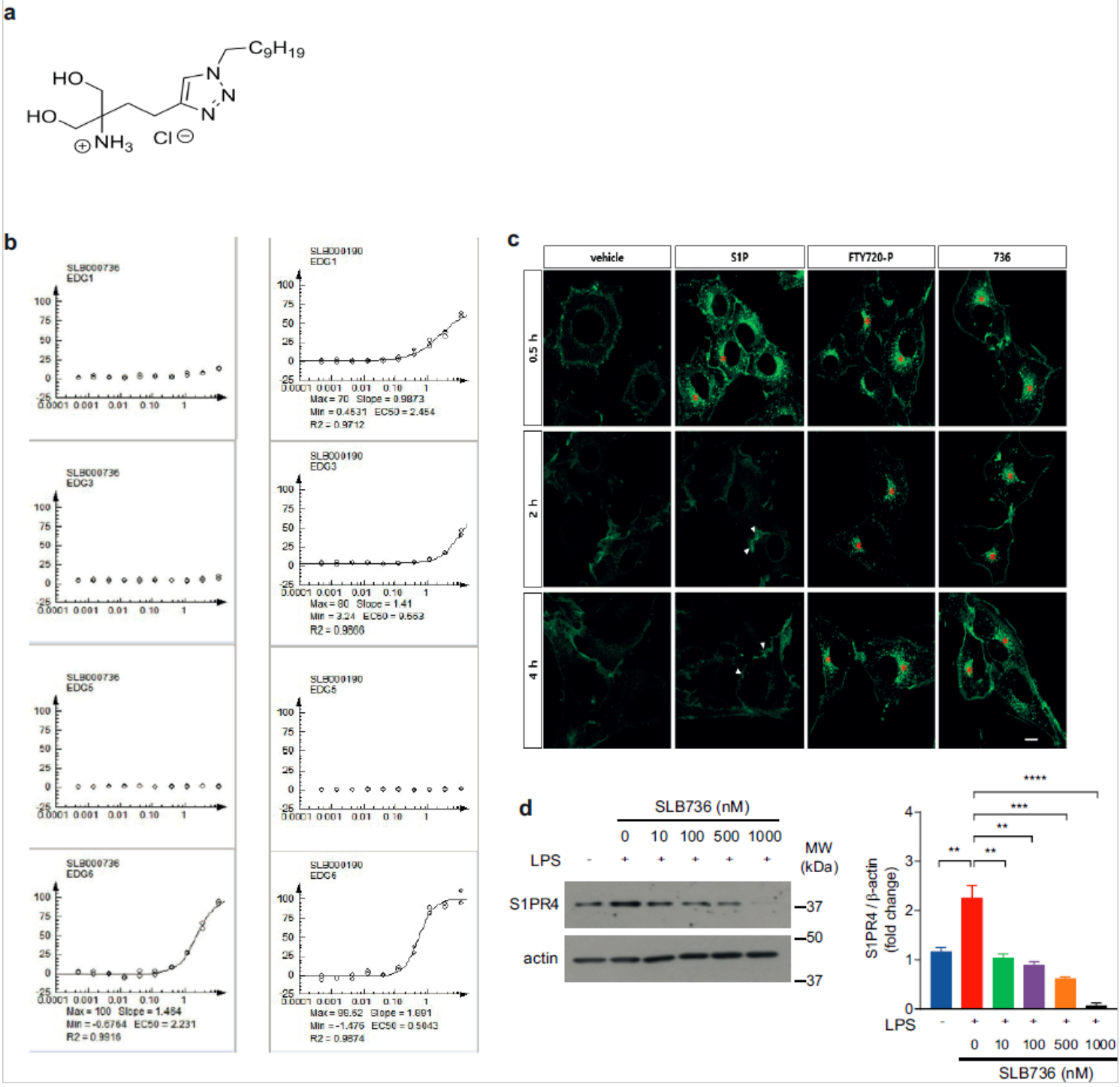

Figure 3

SLB736 acts as a functional antagonist of S1PR4. a Structure of SLB736. b Isoform-specific S1PR activity of SLB736. β-Arrestin PathHunter® assay was performed in the clonal S1PR/HEK293 cell line in the presence of SLB736 (left) and FTY720-P (right). EDG 1 = S1PR1, EDG5 = S1PR2, EDG3 = S1PR3, EDG6 = S1PR4. c S1PR4 internalization and recycling were assessed in C6 glioma cells overexpressing EGFP-fused S1PR4. Cells were exposed to vehicle (0.1% BSA), S1P (100 nM), FTY720-P (1 μM), or SLB736 (1 μM) for 0.5 h and fixed. Cells exposed to reagents for 0.5 h were washed and further incubated with vehicle in the presence of cycloheximide up to 4 h. Asterisks or arrowheads indicate cytosolic locations or the cell surface. Scale bar, 10 μm. d Protein level of S1PR4 in Kupffer cells. Kupffer cells were pre-treated with SLB736 at the indicated dose and then treated with 100 ng/ml of LPS for 24 h (n = 4). All data are shown as mean ± SEM. Data in d were analyzed by one-way ANOVA followed by Tukey's multiple comparisons test. **p < 0.01, ***p < 0.001, ****p < 0.0001.

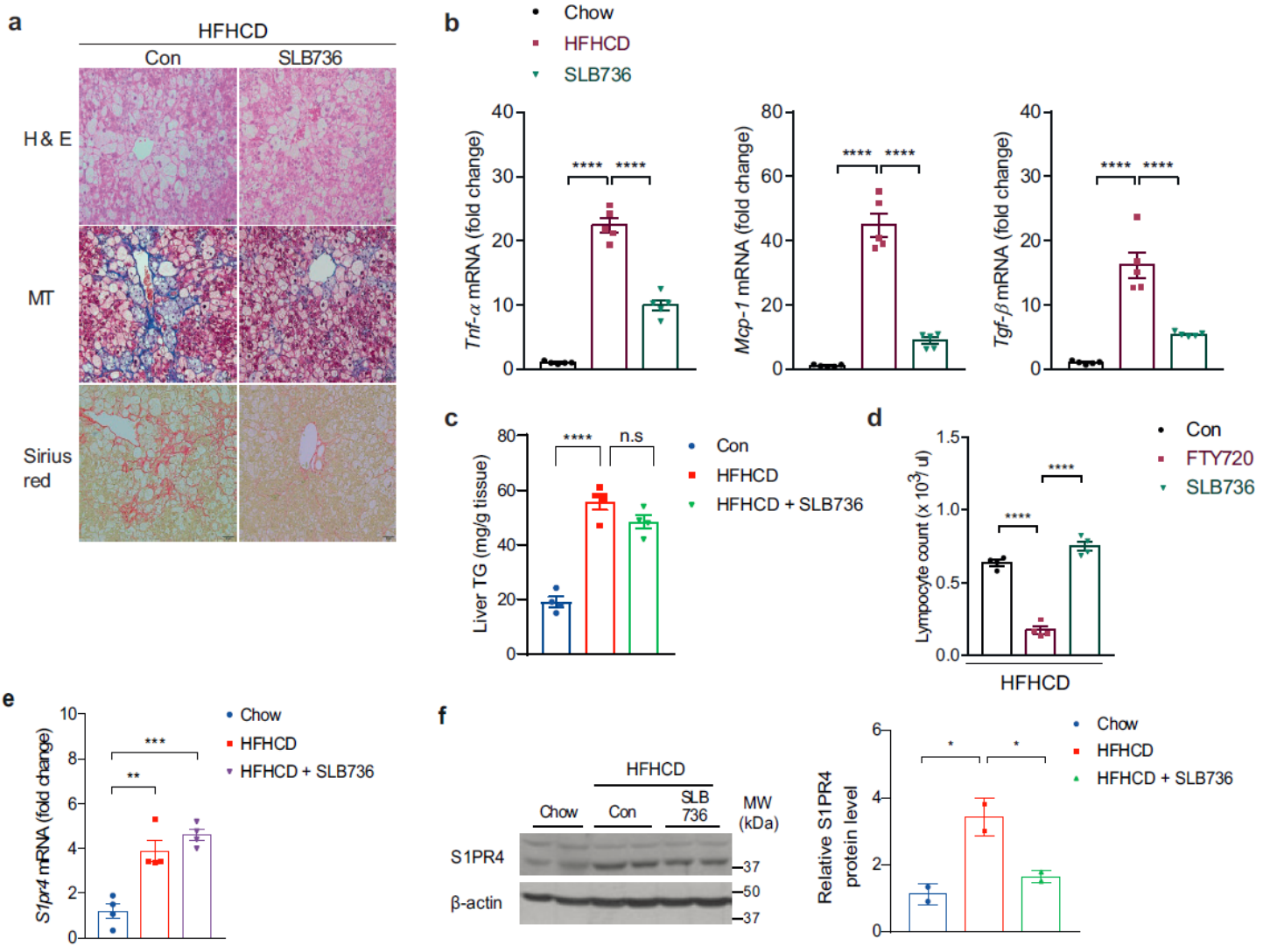

Figure 4

SLB736 treatment prevents HFHCD-induced NASH. a Representative H&E, MT, and Sirius Red staining of the livers. Scale bars, 50 μm. SLB736 (1 mg/kg/day) was administered for 12 weeks in HFHCD-fed mice. b Relative mRNA expression levels of the genes associated with inflammation and fibrosis (n = 5) in the livers of HFHCD-fed mice with or without SLB736 treatment. c TG contents in the livers of HFHCD-fed mice with or without SLB736 treatment (n = 4). d Lymphocyte counts in the blood. FTY720 or SLB736 (1 mg/kg/day) were administered for 12 weeks in HFHCD-fed mice (n = 4). e, f mRNA expression of S1pr4 (e) and representative Western blots of S1PR4 (f) in the liver of HFHCD-fed mice treated with SLB736 (n = 4). All data are shown as mean ± SEM. Data in b, c, d, e and f were analyzed by one-way ANOVA followed by Tukey's multiple comparisons test. *p < 0.05, **p < 0.01, ***p < 0.001, ****p < 0.0001, n.s., not significant.

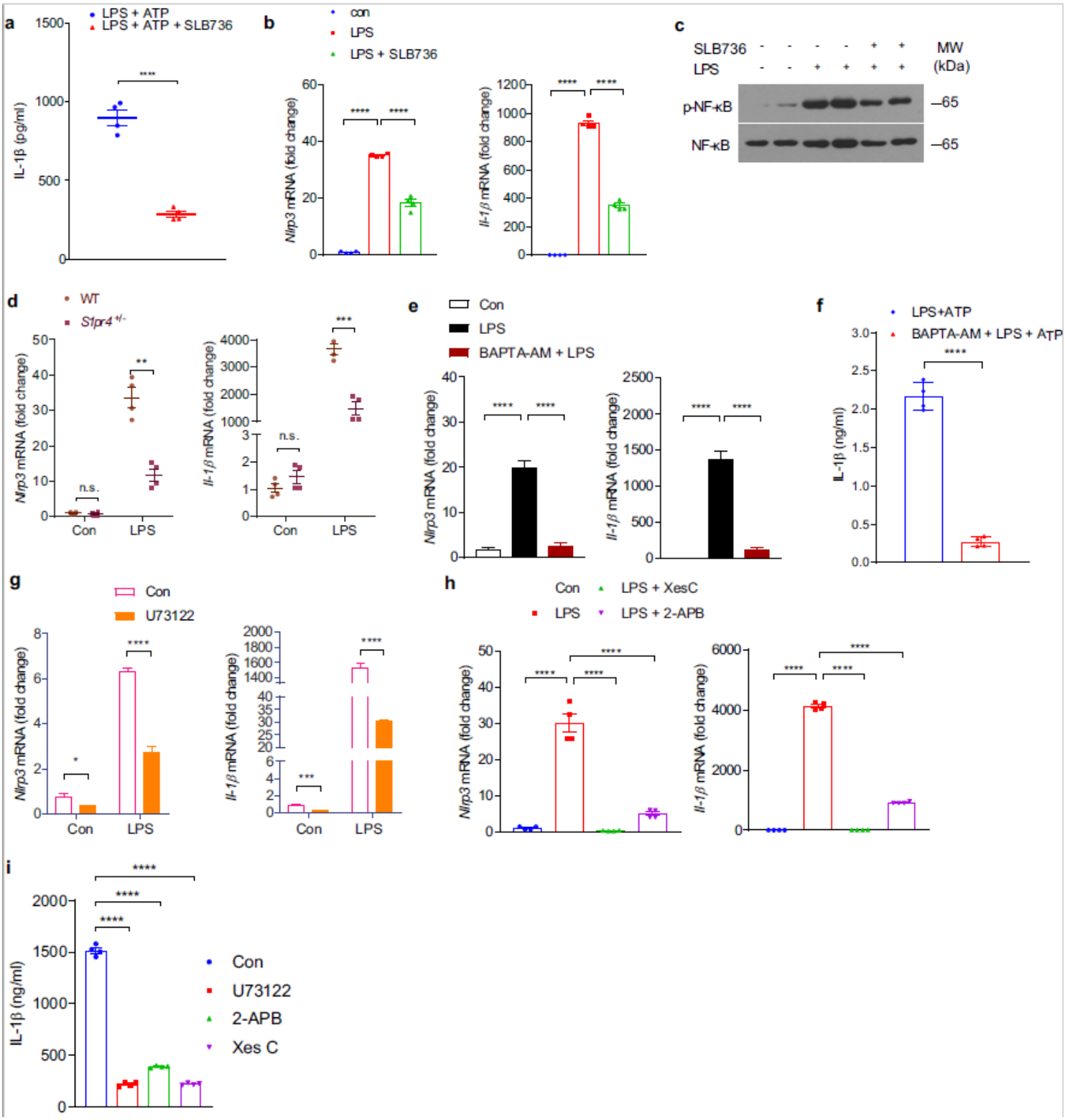

Figure 5

S1pr4 depletion decreases NLRP3 inflammasome activation in Kupffer cells. a, IL-1β levels in the culture media of Kupffer cells. Kupffer cells were pre-treated with 1 μM SLB736 for 2 h, and treated with LPS 100 ng/ ml for 3 h followed by ATP (1 mM) for 30 min. b, c SLB736 decreases the priming of NLRP3 inflammasome activation. Relative mRNA expression of Nlrp3 and Il-1β (b) and representative Western Blots of NF-kB phosphorylation (n = 4) (c). Kupffer cells were pre-treated with 1 μM SLB736 for 2 h, and

treated with LPS 100 ng/ ml for 3 h for the measurement of mRNA expression of Nlrp3 and Il-1β (b), or for 30 min for the measurement of NF-kB phosphorylation (c). d S1pr4 deficiency decreases the priming of NLRP3 inflammasome activation. Kupffer cells isolated from S1pr4 +/- mice were stimulated with LPS (100 ng/ml) for 3 h. Relative mRNA expression levels of Nlrp3 and Il-1β (n = 4). e, f Kupffer cells were pre-treated with BAPTA-AM (10 μM) for 30 min and then treated with LPS (100 ng/mL) for 3 h (e). In another set of experiments, LPS-primed Kupffer cells were treated with ATP (1 mM) for 30 min (f). e Relative mRNA expression levels of Nlrp3 and Il-1β in the cells. f IL-1β secretion into the culture medium (n = 4). g, h Inhibition of LPS-induced Nlrp3 and Il-1β expression by suppression of the PLC/IP3/IP3R axis. Relative mRNA expression levels of Nlrp3 and Il-1β. Kupffer cells were treated with 10 μM U73122, 5 μM Xes C, or 100 μM 2-APB (n = 4). i IL-1β in the culture medium. Kupffer cells pre-treated with U73122 (10 μM), 2-APB (100 μM), Xes C (5 μM), or DMSO (vehicle control) for 30 min. Kupffer cells were treated with 1 mM ATP for 30 min after 3 h of LPS priming (100 ng/mL). IL-1β secreted in the culture supernatants was quantified by ELISA (n = 4). All data are shown as mean ± SEM. All data are shown as mean ± SEM. Data in a, f and g were analyzed by two-tailed Student's t-test. Data in b, e, h and i were analyzed by one-way ANOVA followed by Tukey's multiple comparisons test. *p < 0.05, **p < 0.01, ***p < 0.001, ****p < 0.0001, n.s, not significant.

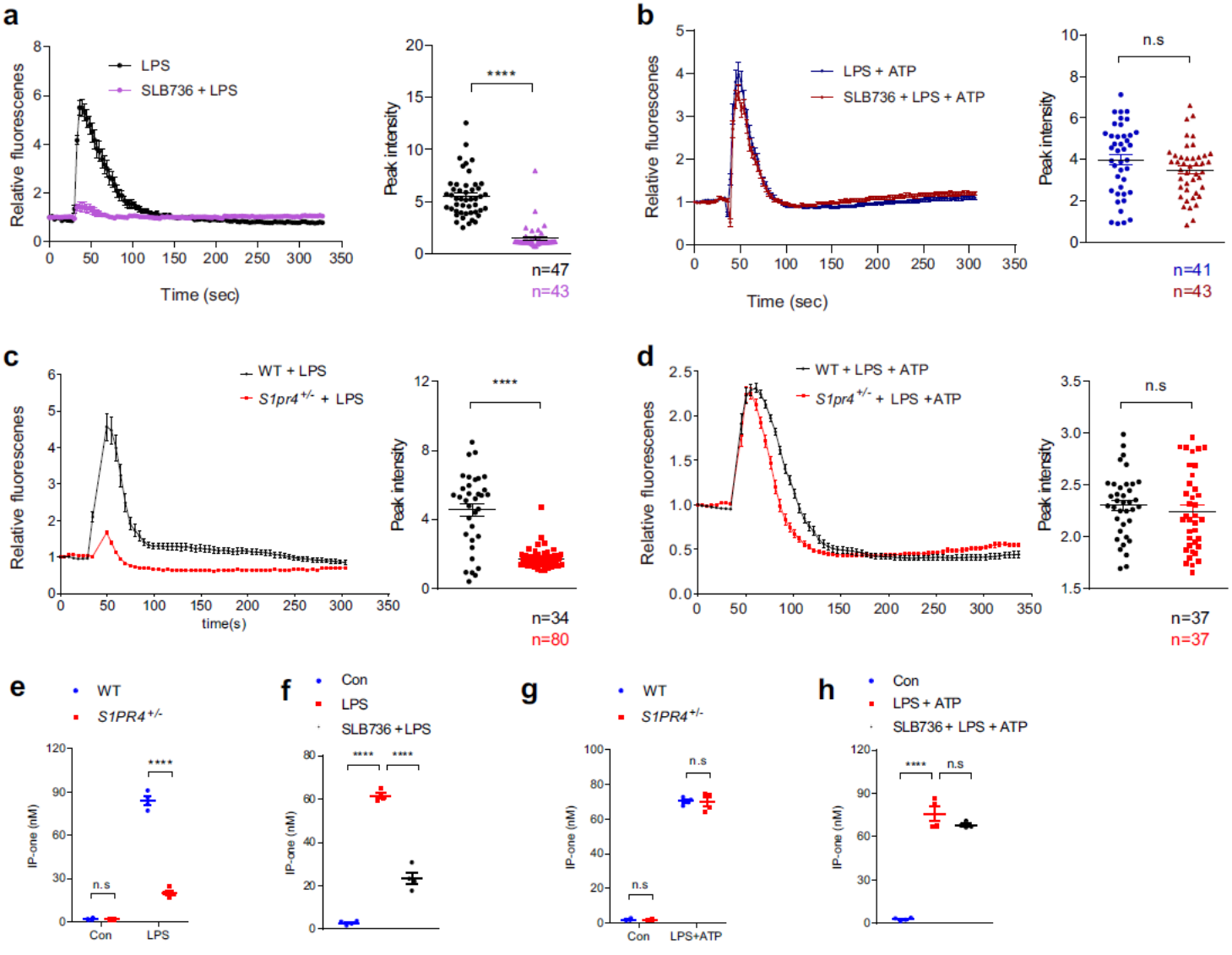

Figure 6

S1PR4 is required for the calcium signalling associated with signal 1 but not signal 2 of the NLRP3 inflammasome activation. a Effect of SLB736 on LPS-mediated [Ca++] release. Kupffer cells were pre-treated with 1 μM SLB736 or vehicle for 2 h. Cells were then incubated with Fluo-4/AM followed by stimulation with LPS. [Ca++] was analyzed by time-lapse confocal microscopy (left panel). Quantification of LPS-induced peak fluorescent intensities (right panel). b Lack of the effect of SLB736 on [Ca++] release in response to ATP in LPS-primed Kupffer cells. Kupffer cells treated with LPS were incubated with 1 μM SLB736 or vehicle for 2 h. The cells were then incubated with Fluo-4/AM followed by stimulation with 1 mM ATP. c, d Changes in [Ca++] in response to LPS and ATP in WT or S1pr4+/- Kupffer cells, with or without LPS-priming. The experimental protocol was the same as that used in a and b. e, f IP-one levels in S1pr4+/- Kupffer cells and SLB736-treated cells (n = 4). The experimental protocol was the same as that used in a and c. g, h IP-one levels in S1pr4+/- Kupffer cells and SLB736-treated cells (n = 4). The experimental protocol was the same as that used in b and d. All data are shown as mean ± SEM. Data in a, b, c, d, e, and g were analyzed by two-tailed Student’s t-test. Data in f and h were analyzed by one-way ANOVA followed by Tukey's multiple comparisons test. ****$p < 0.0001$, n.s., not significant.

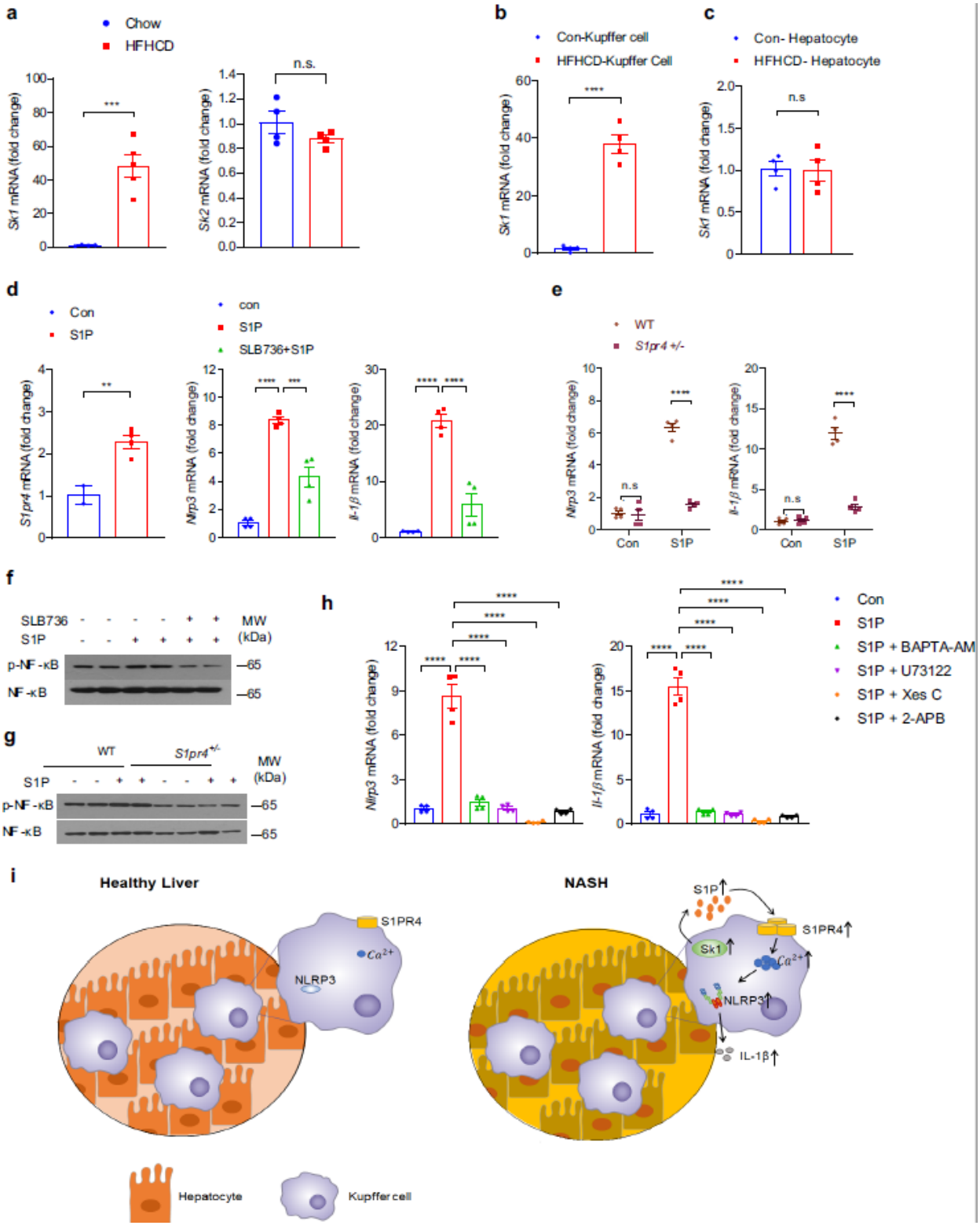

Figure 7

S1P activates NLRP3 inflammasome through S1PR4. a Sk1 and Sk2 mRNA expression in the livers of mice fed HFHCD for 12 weeks (n = 4). b, c Sk1 mRNA expression in primary Kupffer cells (b), and primary hepatocytes (c) from mice fed HFHCD for 4 weeks (n = 4). d S1P-induced priming of NLRP3 inflammasome is decreased by SLB736 treatment. Relative mRNA expression levels of S1pr4, Nlrp3, and Il-1β. Kupffer cells were pre-treated with 1 μM SLB736 for 2 h, and then treated with 40 μM of S1P for 3 h

(n = 4). e S1pr4 knockdown decreases S1P-induced priming of NLRP3 inflammasome activation. Relative mRNA expression of Nlrp3 and Il-1β. S1pr4+/- Kupffer cells were treated with S1P (40 μM) for 3 h (n = 4). f, g Representative Western Blots of NF-kB phosphorylation. Kupffer cells were pre-treated with SLB736 (1 μM) for 2 h, and then treated with S1P (10 μM) for 30 min (n = 3). h mRNA expression of Nlrp3 and Il-1β. Kupffer cells were treated with BAPTA-AM (10 μM), U73122 (10 μM), Xes C (5 μM), or 2-APB (100 μM), and treated with S1P (40 μM) (n = 4). i Conceptual model depicting the role of the SK1/S1PR4 axis in the pathogenesis of NASH. S1P produced by SK1 from Kupffer cells induces S1PR4 in a paracrine manner, which is necessary for the [Ca++]-dependent priming of the NLRP3 inflammasome. All data are shown as mean ± SEM. Data in a, b, c and e were analyzed by two-tailed Student's t-test. Data in d and h were analyzed by one-way ANOVA followed by Tukey's multiple comparisons test. **p < 0.01, ***p < 0.001, ****p < 0.0001, n.s., not significant.

Supplementary Files

This is a list of supplementary files associated with this preprint. Click to download.

- SupplementaryMovieS1.mov
- SupplementaryMovieS2.mov
- SupplementaryMovieS3.mov
- SupplementaryMovieS4.mov
- SupplementaryMovieS5.mov
- SupplementaryMovieS6.mov
- SupplementaryMovieS7.mov
- SupplementaryMovieS8.mov
- SupportingData.pdf